Journal of Sound and Vibration (2000) **233**(1), 119–135
doi:10.1006/jsvi.1999.2793, available online at http://www.idealibrary.com on IDEAL®

EFFECT OF A CRACK ON THE DYNAMIC STABILITY OF A FREE–FREE BEAM SUBJECTED TO A FOLLOWER FORCE

K.-H. KIM AND J.-H. KIM

Department of Aerospace Engineering, Seoul National University, Seoul 151-742, *Korea*

(*Received* 25 *March* 1999, *and in final form* 22 *November* 1999)

In the present study, the effect of a crack on the dynamic stability of a free–free Timoshenko beam is investigated when it is subjected to a constant or a pulsating follower force. A crack, one of the structural damages, results in a change of transverse vibration frequencies and mode shapes. In addition, the crack may change the stability characteristics of the beam. A mathematical model for the crack is introduced in the form of the bending and shear compliance of equivalent incremental strain energy. To obtain numerical results, the finite element method and the method of multiple scales are applied in this work. As a conclusion, the effect of the crack location and depth on the stability characteristics of the system is illustrated.

1. INTRODUCTION

A free–free beam subjected to a follower force has been extensively studied for the modelling and analysis of dynamic stability of flexible missiles or space structures. The follower force has been treated as a typical example of non-conservative force as in reference [1]. A large amount of research work dealing with the analysis of this kind of problems has been carried out. Beal [2] investigated the dynamic stability of a missile, as was modelled by a beam subjected to a thrust. In the paper, Galerkin's method of analysis was used and then the stability characteristics of a beam was studied when it was subjected to a constant and pulsating follower force. Wu [3] used the finite element method for the dynamic stability analysis of a missile under a follower force. It was noted that the eigenvalue for the rigid-body mode became considerably large in the unstable regions. Higuchi [4] studied the free–free beam with an end thrust. He compared the experimental data with the numerical results for the dynamic stability analysis, and noted that the results were approximately equal to each other. In case of the follower force with a pulsating part, it may cause an instability due to "parametric resonance". As a matter of fact, a considerably weak force may result in structural instability around a specific frequency of the pulsating part of a force. Kar and Sujata [5] studied the dynamic stability of a rotating beam under a transverse pulsating excitation. Using the method of multiple scales, they showed that the first order approximation was quite accurate. Kim and Choo [6] studied the dynamic stability of a free–free beam with a concentrated mass subjected to a constant and pulsating follower force. In this research work, by the finite element method and the method of multiple scales, the concentrated mass may change the combination-resonance type and the regions of instability.

0022-460X/00/210119 + 17 $35.00/0

It is well known that a crack may change the dynamic characteristics of a structure. In other words, the crack results in the deviation of frequencies and mode shapes for the vibration. In the past 20 years, the effect of a crack on structural vibration has been studied by experiments or numerical methods of analysis. Due to the simplicity in the analysis of the crack, the equivalent mathematical compliance has been widely used for numerical studies. This method of analysis has been widely used, and many studies using this method have been published. Anifantis and Dimarogonas [7] studied the effect of a crack on the stability of a clamped beam subjected to a follower force. The equivalent spring model was used to substitute a crack and it was shown that the crack changed eigenvalue curves and critical loads. Gounaris and Dimarogonas [8] suggested a method in which the flexibility matrix can be used in the finite element model. Suace *et al.* [9] studied the vibration of a cantilever beam with a crack. In this work, they only considered breathing mode of the crack, and obtained non-linear solution by considering time-dependent crack conditions. Qian *et al.* [10] compared the opening crack model with the breathing crack model. They concluded that the difference of solutions between the two models was quite small when the amplitude was not so large, and the difference became large as the amplitude increased.

Changes in vibration characteristics may result in changes in stability characteristics. This means that the crack may change the critical loads or instability types. In the present study, the effect of the crack on the stability of the free–free Timoshenko beam is investigated when it is subjected to a constant and a pulsating follower force. The finite element method and the method of multiples are employed to obtain numerical data. For convenience, the crack in this study is substituted by the equivalent flexibility matrix obtained by equivalent increased strain energy and strain energy density function from fracture mechanics [11]. For the various depths and locations of the cracks, the changes in the critical load and the instability type are investigated. In the case of the pulsating follower force, the change in the region of parametric resonance is investigated by the first order expansion of the method of multiple scales.

2. ANALYSIS

2.1. FINITE ELEMENT ANALYSIS

Figure 1 shows a mathematical model to be used in this study. As shown in Figure 1(a), consider a beam of length L with a crack at x_c subjected to a pulsating follower force $P = P_0 + P_1 \cos \Omega t$. Figure 1(b) shows a circular cross-section of radius r, and diameter h with a crack on which moments and shear forces are acting. Based on the Timoshenko beam theory, the strain–displacement relation is expressed as in reference [12],

$$\varepsilon_{xx} = -\, y\theta_{,x},$$

$$\gamma_{xy} = w_{,x} - \theta, \tag{1}$$

where w and θ are the deflection in y axis and rotation in xy plane respectively.

Hamilton's principle is used to derive equations of motion for the beam model as

$$\delta \int_{t_1}^{t_2} (T - U + W_c)\, \mathrm{d}t + \int_{t_1}^{t_2} \delta W_{nc}\, \mathrm{d}t = 0. \tag{2}$$

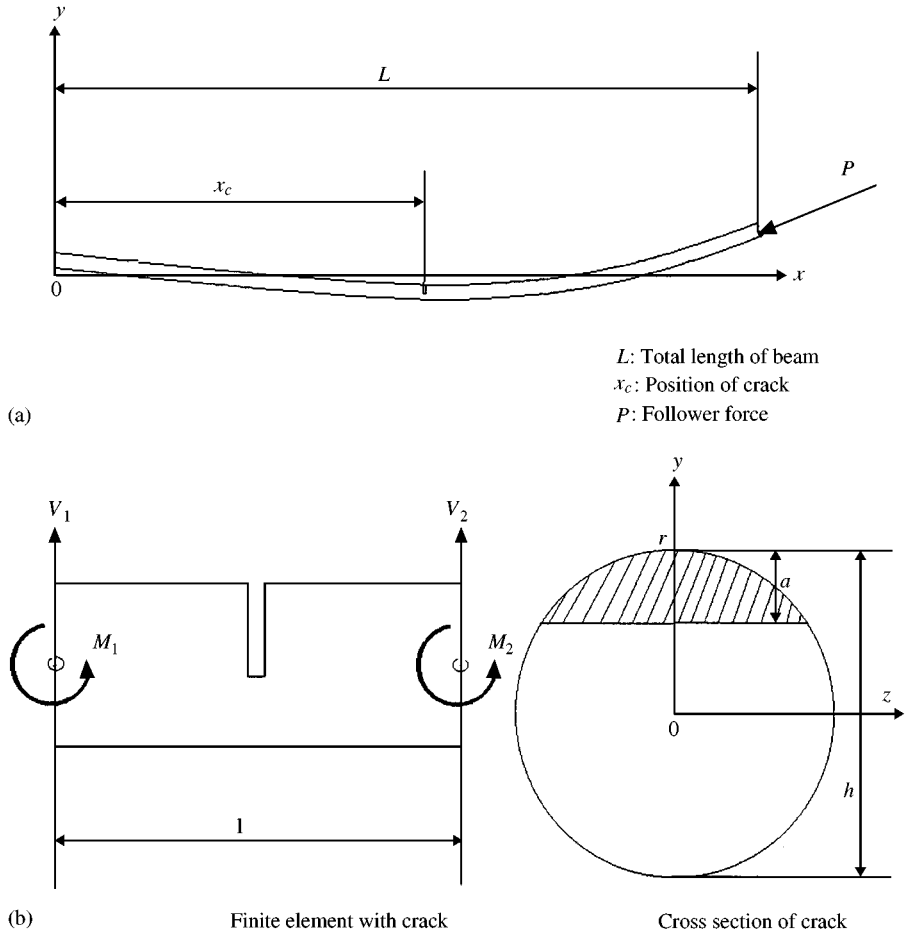

Figure 1. Mathematical model. (a) Free-free beam with a crack subjected to a follower force; (b) element with a crack.

The strain energy U is given by

$$U = \frac{1}{2}\int_V (\varepsilon_{xx}\tau_{xx} + \gamma_{xy}\tau_{xy})\,\mathrm{dV}$$

$$= \frac{1}{2}\int_0^L EI\theta_{,x}^2 + \frac{1}{2}\int_0^L kGA(w_{,x} - \theta)^2\,\mathrm{d}x, \tag{3}$$

where E means Young's modulus, I denotes the moment of inertia of the cross-section, k stands for the shear correction factor, G means the shear modulus and A denotes the area of the cross-section. In addition, EI and kGA mean the bending stiffness and the shear stiffness respectively. The kinetic energy T is given by

$$T = \frac{1}{2}\int_0^L \rho A\dot{w}^2\,\mathrm{d}x + \frac{1}{2}\int_0^L \rho I\dot{\theta}^2\,\mathrm{d}x, \tag{4}$$

where ρ is the mass per unit volume. The work W_c by the longitudinal component of a follower force is

$$W_c = \frac{1}{2}\int_0^L (P_0 + P_1 \cos \Omega t)\frac{x}{L} w_{,x}^2 \, \mathrm{d}x. \tag{5}$$

The virtual work δW_{nc} due to the transverse component of a follower force is

$$\delta W_{nc} = -(P_0 + P_1 \cos \Omega t) w_{,x}|_{X=L} \delta w. \tag{6}$$

Now, we use the following non-dimensional parameters, and governing equations are discretized by the improved 2-node element (see reference [13] for details),

$$R = \frac{I}{AL^2}, \quad S = \frac{kAGL^2}{EI}, \quad \tau = \frac{1}{L^2}\sqrt{\frac{EI}{\rho A}}\, t,$$

$$Q_0 = \frac{P_0 L^2}{EI}, \quad Q_1 = \frac{P_1 L^2}{EI}, \quad \omega^2 = \frac{\rho A L^4}{EI}\lambda^2, \quad \bar{\Omega}^2 = \frac{\rho A L^4}{EI}\Omega^2, \tag{7}$$

where $x' = x - (i-1)l$ at the ith element, $k = 6(1+\nu)/(7+6\nu)$ with l being the size of the element, ν is the Poisson ratio and ω is non-dimensional frequency. Discretized and assembled in the whole domain, the equations are given in the form

$$\mathbf{M}\{\ddot{\mathbf{U}}\} + (\mathbf{K}_b - Q_0\mathbf{K}_f)\{\mathbf{U}\} - Q_1 \cos \bar{\Omega}\tau \mathbf{K}_f\{\mathbf{U}\} = \{0\}, \tag{8}$$

where $\mathbf{M}$ is the mass matrix, $\mathbf{K}_b$ is the bending stiffness matrix and $\mathbf{K}_f$ is the geometric matrix due to the follower force.

2.2. MATHEMATICAL MODEL OF THE CRACK

The additional strain energy due to the crack can be considered in the form of a flexibility coefficient expressed in terms of the stress intensity factor, which can be derived by Castigliano's theorem in the linear elastic range. An approach to this kind of problem is one in which the element with a crack is constrained at one side and then the forces are applied at the other side. The flexibility matrix can be easily obtained, and the stiffness matrix of the element with a crack can be derived from the conditions of equilibrium. The term $c_{ij}^{(1)}$ of the additional flexibility matrix $\mathbf{C}(1)$ due to the crack can be formulated as

$$c_{ij}^{(1)} = \frac{\partial U}{\partial P_j} = \frac{\partial^2}{\partial P_i \partial P_j}\iint_S J \, \mathrm{d}S, \tag{9}$$

where J is the strain energy density function, and the total strain energy due to the crack can be determined by integrating J over the crack. In addition, U_i is the displacement and P_i is the force in the i direction. The strain energy density function can be expressed as a function of the stress intensity factor as

$$J = \frac{1}{E'}\left[\left(\sum_{i=1}^{6} K_{\mathrm{I}i}\right)^2 + \left(\sum_{i=1}^{6} K_{\mathrm{II}i}\right)^2 + \left(\sum_{i=1}^{6} K_{\mathrm{III}i}\right)^2\right], \tag{10}$$

where $E' = E/(1 + \nu)$. In addition, $K_{\mathrm{I}i}$ denotes the opening-type mode, $K_{\mathrm{II}i}$ stands for the sliding-type mode and $K_{\mathrm{III}i}$ represents the tearing-type mode.

For the transverse bending mode, the strain energy density function is given in terms of the stress intensity factor as

$$J = \frac{1}{E'}[(K_{\mathrm{I}M} + K_{\mathrm{I}P})^2 + K_{\mathrm{II}P}^2], \tag{11}$$

where $K_{\mathrm{I}M}$ denotes opening-type mode by moment, $K_{\mathrm{I}P}$ stands for opening-type mode by shear force, and $K_{\mathrm{II}P}$ represents sliding-type mode by shear force. For the convenience of integration over the circular cross-section, the stress intensity factors are modified and expressed as

$$K_{\mathrm{I}P} = \frac{2V}{\pi r^4} l \sqrt{r^2 - x^2}\sqrt{\pi y} F_{\mathrm{I}}(y/h),$$

$$K_{\mathrm{I}M} = \frac{4M}{\pi r^4} \sqrt{r^2 - x^2}\sqrt{\pi y} F_{\mathrm{I}}(y/h),$$

$$K_{\mathrm{II}P} = \frac{kV}{\pi r^2} \sqrt{\pi y} F_{\mathrm{II}}(y/h), \tag{12}$$

where V, M denote force and moment, respectively, and

$$F_{\mathrm{I}}(y/h) = (\tan \xi/\xi)^{1/2}[0{\cdot}923 + 0{\cdot}199(1 - \sin \xi)^4]/\cos \xi,$$

$$F_{II}(y/h) = [1{\cdot}122 - 0{\cdot}561(y/h) + 0{\cdot}085(y/h)^2 + 0{\cdot}18(y/h)^3]/(1 - y/h)^{1/2}$$

with $\xi = \pi y/(2h)$. Substituting equations (11) and (12) into equation (9), the flexible matrix due to the crack can be obtained.

The flexibility matrix for the element without a crack is represented by $\mathbf{C}(0)$. From the equilibrium condition as shown in Figure 1(b), the transformation matrix $\bar{T}$, the stiffness matrix of the element without crack can be obtained as

$$\{V_i, M_i, V_{i+1}, M_{i+1}\}^{\mathrm{T}} = \bar{T} = \{V_{i+1}, M_{i+1}\}. \tag{13}$$

Using the flexibility matrix and transformation matrix $\bar{T}$, the stiffness matrix of the element without crack can be obtained as follows:

$$EK_{bc} = \bar{T}(C^{(0)} + C^{(1)})^{-1}\bar{T}^{\mathrm{T}}, \tag{14}$$

where EK_{bc} is the stiffness matrix of the element containing the crack.

2.3. METHOD OF ANALYSIS

The discretized equations of motion are given by equation (8). We can write it in the form

$$\mathbf{M}\{\ddot{\mathbf{U}}\} + \mathbf{K}\{\mathbf{U}\} - \beta Q_{cr} \cos \bar{\Omega}\tau \mathbf{K}_f\{\mathbf{U}\} = \{0\}, \tag{15}$$

where $\beta = Q_1/Q_{cr}$ and $\mathbf{K} = \mathbf{K}_b - Q_0\mathbf{K}_f$ noting that Q_{cr} is the critical load of a beam without a crack under a constant follower force. Applying the modal transformation, we can transform the matrices $\mathbf{M}$ and $\mathbf{K}$ into diagonal matrices simultaneously, and then we can use the method of multiple scales for the stability analysis.

Now, the mathematical processes are summarized. First of all, in order to exclude the effect of the rigid body mode, only the modal vectors that represent the elastic modes are used in the transformation. Adopting the normalized right modal matrix Φ, one gets the following equations by transforming $\{\mathbf{U}\}$ to $\Phi\{\boldsymbol{\eta}\}$, and multiplying the transposed left modal matrix Ψ^{T}:

$$\mathbf{I}\{\ddot{\eta}\} + \mathbf{\Lambda}\{\eta\} - \beta Q_{cr}\cos\bar{\Omega}\tau\mathbf{R}\{\eta\} = \{0\}, \tag{16}$$

where $\Psi^{\mathrm{T}}\mathbf{M}\mathbf{\Phi} = \mathbf{I}$, $\Psi^{\mathrm{T}}\mathbf{K}\Phi = \Lambda$, $\Psi^{\mathrm{T}}\mathbf{K}_f\mathbf{\Phi} = \mathbf{R}$ and $\mathbf{I}$ is identity matrix. Rewriting the above equation in component form, we have

$$\ddot{\eta}_j + \omega_j^2\eta_j + 2\varepsilon\cos\bar{\Omega}\tau\sum_{m=1}^{n-2}\tilde{R}_{jm}\eta_m = 0, \tag{17}$$

where $\varepsilon = -\beta/2$, $\tilde{R}_{jm} = R_{jm}Q_{cr}$.

According to the method of multiple scales, the solution can be expressed in terms of ε as follows:

$$\eta_j(t,\varepsilon) = \eta_{j0}(T_0, T_1, T_2, \ldots) + \varepsilon\eta_{j1}(T_0, T_1, T_2, \ldots) + \varepsilon^2\eta_{j2}(T_0, T_1, T_2, \ldots) + \cdots, \tag{18}$$

where $T_n = \varepsilon^n t$, $n = 0, 1, 2, \ldots$. Through the first order approximation, we can obtain the transition curves in the ε–$\bar{\Omega}$ plane as follows (see reference [14] for details):

(a) *Sum-type combination resonance*:

$$\bar{\Omega} = \omega_p + \omega_q \pm \varepsilon[\tilde{R}_{pq}\tilde{R}_{qp}/\omega_p\omega_q]^{1/2} + O(\varepsilon^2). \tag{19.1}$$

(b) *Difference-type combination resonance*:

$$\bar{\Omega} = \omega_p - \omega_q \pm \varepsilon[-\tilde{R}_{pq}\tilde{R}_{qp}/\omega_p\omega_q]^{1/2} + O(\varepsilon^2). \tag{19.2}$$

The sum-type and difference-type combination resonances cannot exist simultaneously. If a force is a conservative type, difference-type combination resonance does not appear as the symmetry of $\mathbf{R}$. For the non-conservative case, $\tilde{R}_{pq}$, $\tilde{R}_{qp}$ can have opposite signs, and the difference-type may also exist. In this study, the variation in instability region in the ε–Ω plane is investigated with varying depths and locations of the crack.

3. NUMERICAL RESULTS AND DISCUSSION

Table 1 shows the non-dimensional frequency reduction due to the crack, the depth of which varies from 0 to 0·4. To check the convergence of the present numerical results, the crack is located at the mid-point of the beam and the results are compared with the analytical solution for a simply supported Euler beam. Because the beam model has quite a large slenderness ratio ($L/h = 300$), it can be compared to the Euler beam. Figures 2 and 3 show frequency reduction of the first and second modes. As shown in the figures, the reduction in frequency is related to the depth and the position of the crack, and the mode shapes.

TABLE 1

Non-dimensional frequency reduction due to a crack located at the mid-point of a simply supported beam

Number of elements	$N = 5$		$N = 15$		$N = 25$		Analytical solution	
Mode Depth (a/h)	1st	2nd	1st	2nd	1st	2nd	1st	2nd
0	9·8705	39·5410	9·8695	39·4770	9·8695	39·4780	9·8696	39·4780
0·1	9·8668	39·5290	9·8657	39·4620	9·8657	39·4610	9·8658	39·4630
0·2	9·8503	39·4750	9·8486	39·3960	9·8486	39·3950	9·8487	39·3950
0·3	9·8147	39·3580	9·8117	39·2520	9·8117	39·2480	9·8117	39·2480
0·4	9·7498	39·1420	9·7450	38·9950	9·7450	38·9880	9·7450	38·9850

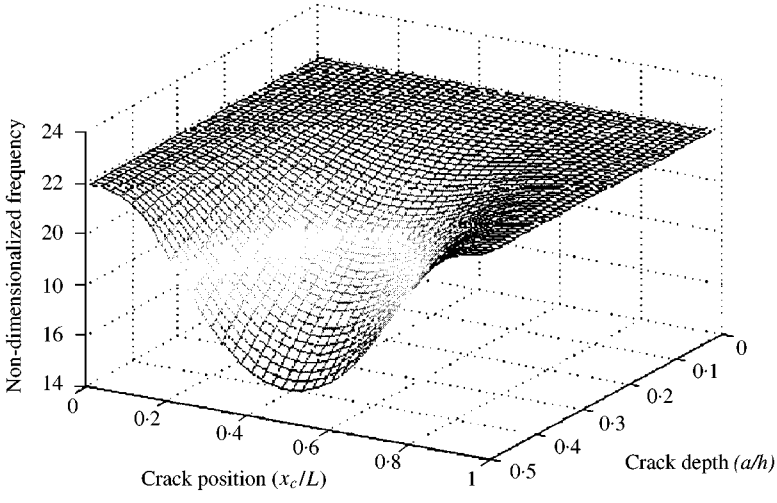

Figure 2. First mode frequency reduction due to a crack.

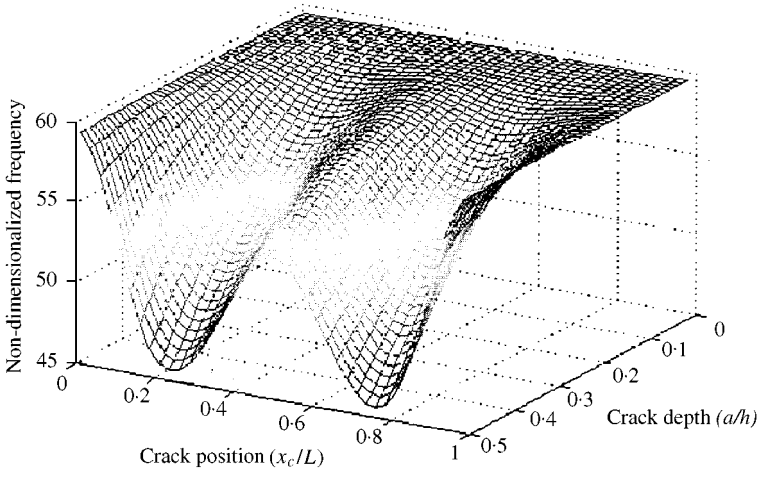

Figure 3. Second mode frequency reduction due to a crack.

3.1. EFFECT OF A CRACK ON THE STABILITY

In this study, all parameters are non-dimensional, and the diameter of the cross-section and the length of the beam are set at a ratio of 1 : 10.

3.1.1. *Constant follower force*

Figure 4(a) shows the variation of eigenvalue curves for $x_c/L = 0{\cdot}1$ (refer to Figure 1(a)). As the follower force increases, the first and the second mode frequencies decrease and finally coincide with each other. Figure 4(b) shows the changes of the critical load as the size

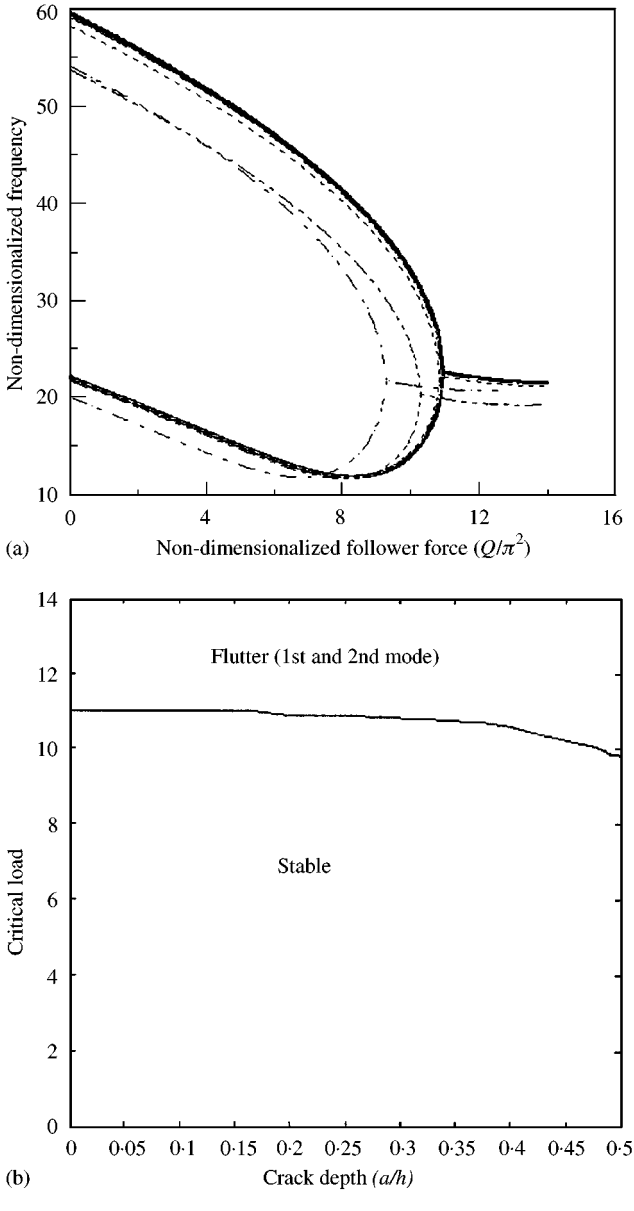

Figure 4. Change of stability characteristics by the crack located at 10% of beam length. (a) Eigenvalue curves. Crack depth (a/h): ——— 0; —— 0·1; —— 0·2; - - - - - 0·3; — - — 0·4; — - - — 0·5. (b) Critical load versus crack depth.

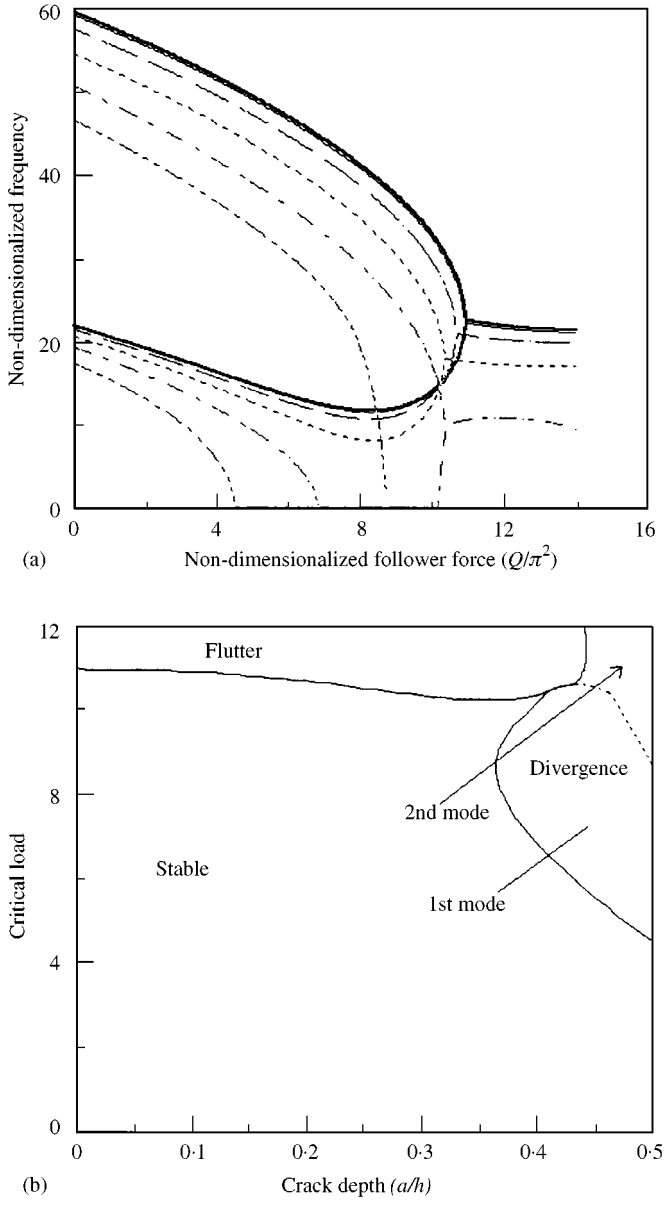

Figure 5. Changes of stability characteristics by the crack located at 30% of beam length. (a) Eigenvalue curves. Crack depth (a/h): ——— 0; —— 0·1; —— 0·2; - - - - - 0·3; — - — 0·4; — - - — 0·5. (b) Critical load versus crack depth.

of the crack increases. The critical load slightly decreases and there is no change in instability type. Figure 5 shows the stability characteristics of the beam for $x_c/L = 0{\cdot}3$. As the depth of the crack becomes 37% of the diameter of the cross-section, the first mode frequency merges into zero and divergence instability occurs. In this case, instability type is divergence and it induces a sudden drop in the critical load. As shown in Figure 6, when the crack is located at the mid-point of the beam, the divergence instability occurs at the shallow crack and the amount of the critical load decrement is conspicuous. When the

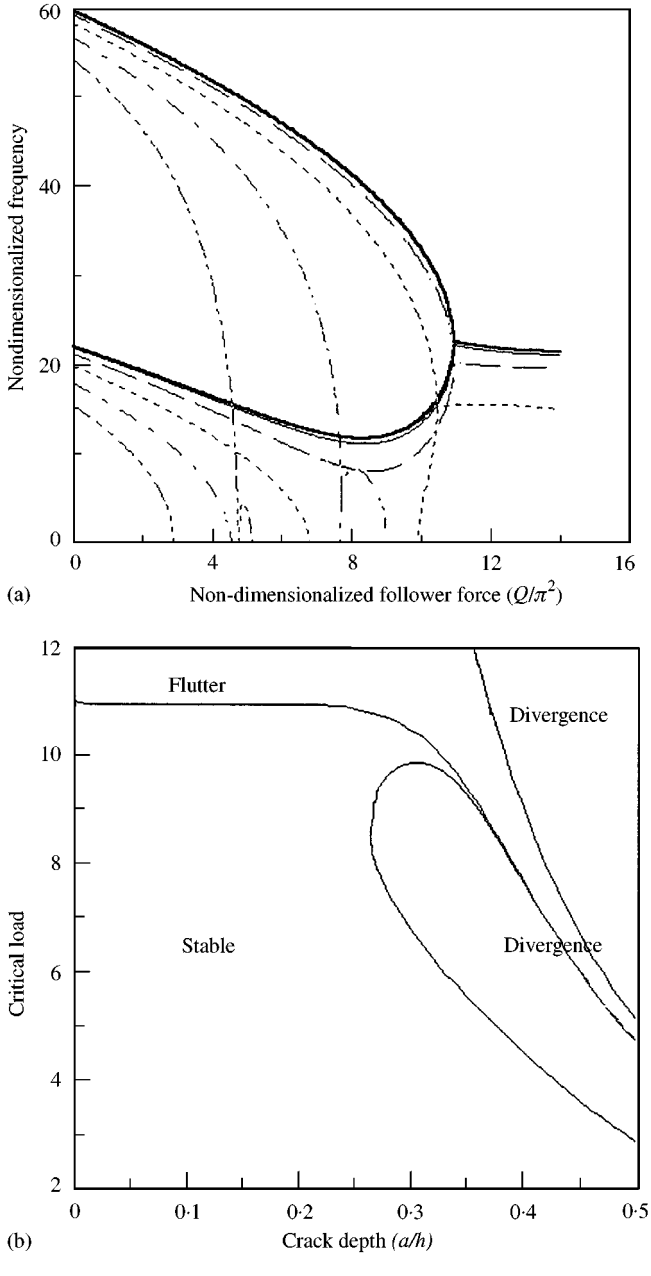

Figure 6. Changes of stability characteristics by the crack located at 50% of beam length. (a) Eigenvalue curves. Crack depth (a/h): ——— 0; —— 0·1; —— 0·2; - - - - - 0·3; — - — 0·4; — - - — 0·5. (b) Critical load versus crack depth.

depth of the crack becomes 50% of the section diameter, the critical load becomes a quarter of the original critical load. Figure 7 shows the stability characteristics of the beam in the case of $x_c/L = 0{\cdot}7$. The critical load decrement of the flutter type is conspicuous and the divergence does not appear. Figure 8 shows the stability characteristics of the beam in the case $x_c/L = 0{\cdot}9$. As for the case of $x_c/L = 0{\cdot}7$, the decrement of the flutter-type critical load is conspicuous. As the depth of the crack becomes about half of the diameter of the cross-

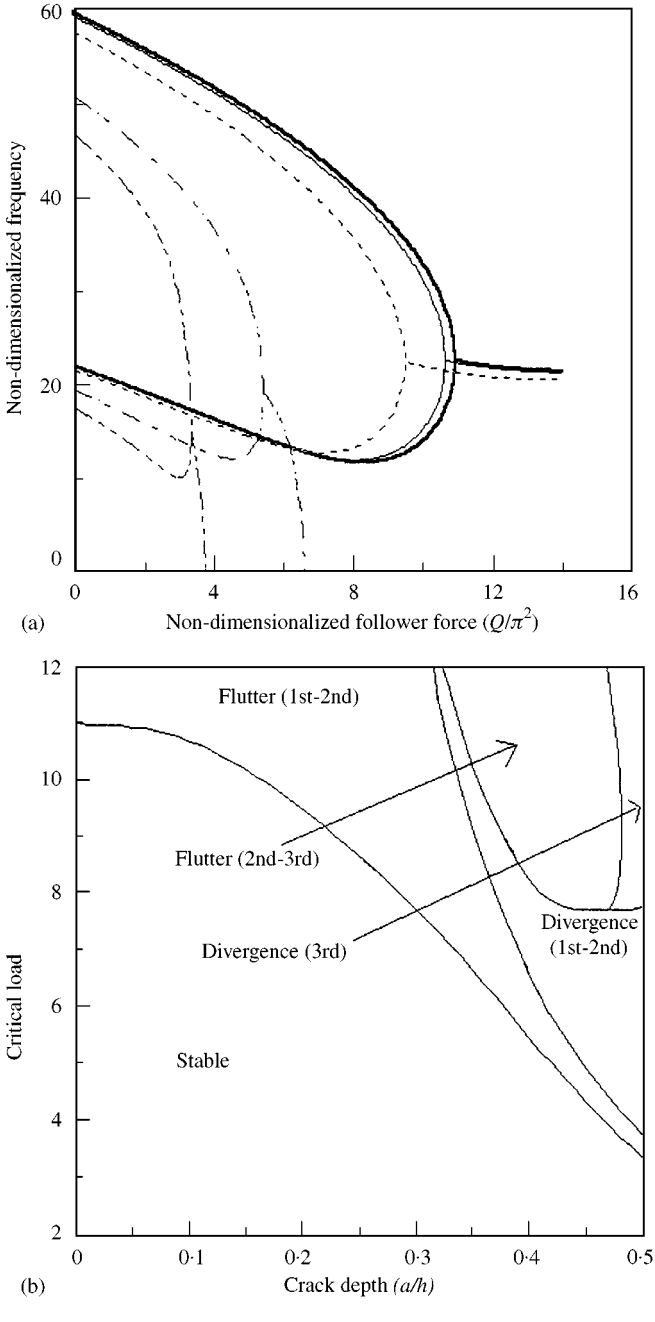

Figure 7. Changes of stability characteristics by the crack located at 70% of beam length. (a) Eigenvalue curves. Crack depth (a/h): ——— 0; —— 0·1; —— 0·2; - - - - - 0·3; — - — 0·4; — - - — 0·5. (b) Critical load versus crack depth.

section, divergence-type instability occurs. Figure 9 shows the influence of the location of the crack on the critical load and the instability type. The divergence-type instability causes a sudden drop in the critical load around the mid-point of the beam, and the effect of the crack is significant as the crack is located at the latter part of the beam. We can conclude

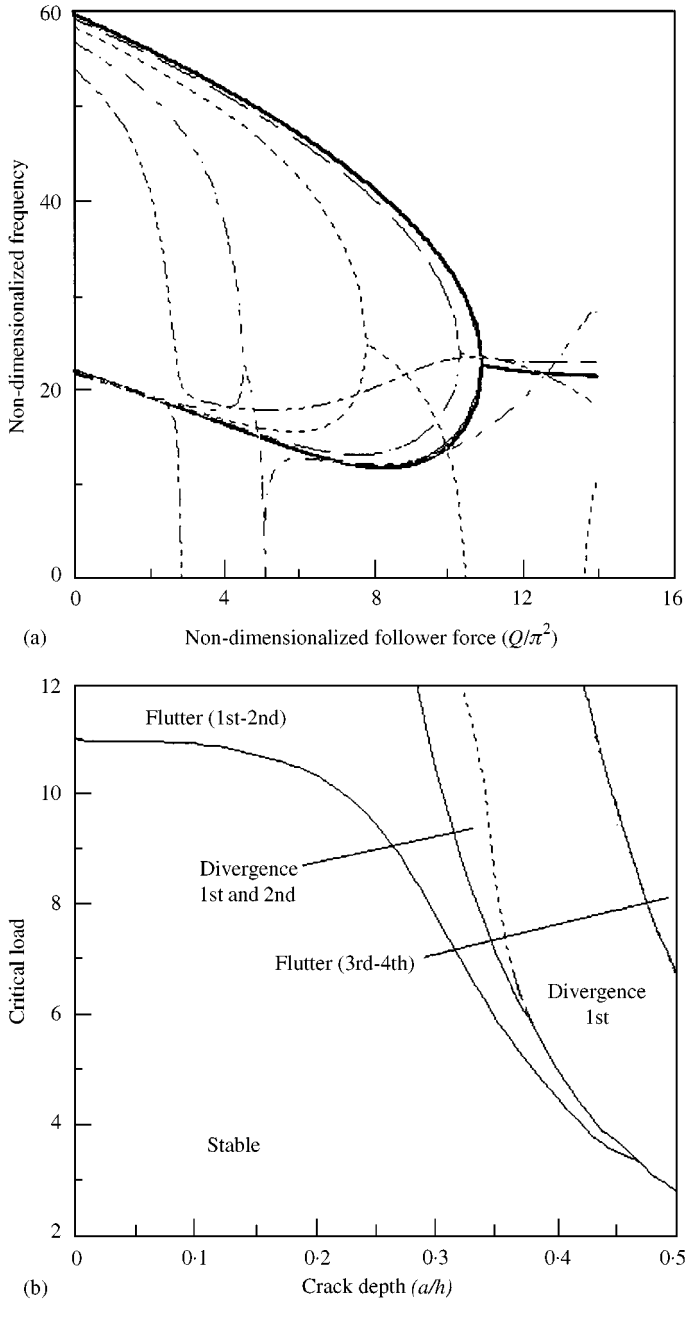

Figure 8. Changes of stability characteristics by the crack located at 90% of beam length. (a) Eigenvalue curves. Crack depth (a/h): ——— 0; —— 0·1; —— 0·2; - - - - - 0·3; — - — 0·4; — - - — 0·5. (b) Critical load versus crack depth.

that the decrement of the flutter-type critical local is mainly dependent on the second mode frequency reduction and the divergence-type instability is largely dependent on the first mode frequency reduction. As a result, the position of the crack is important for the type of instability and vibration mode shapes.

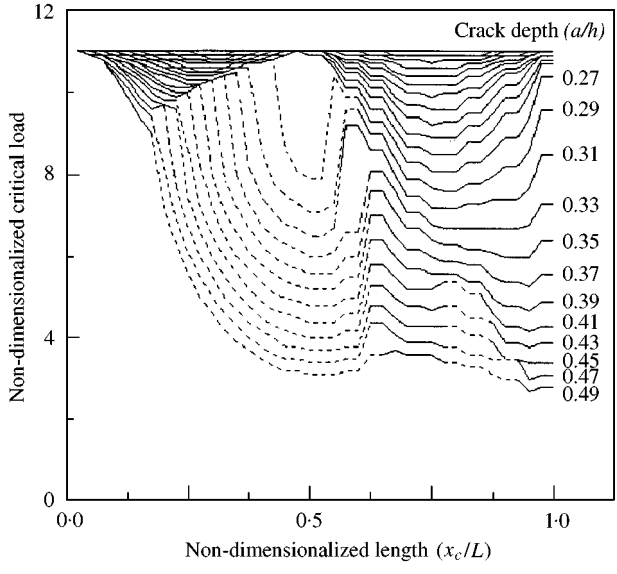

Figure 9. Changes of the critical load due to the crack. ——— Flutter; – – – – Divergence.

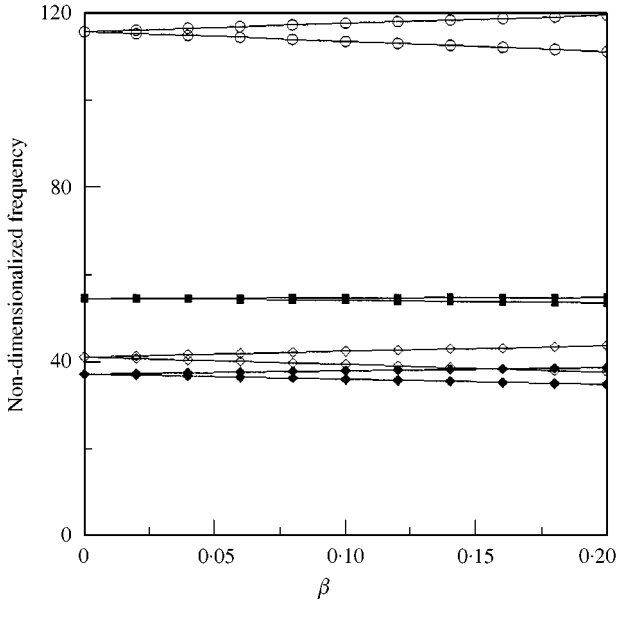

Figure 10. Parametric instability region of the beam without a crack. —○— $2\omega 2$; —◆— $\omega 2$–$\omega 1$; —■— $\omega 3$–$\omega 2$; —◇— $2\omega 1$.

3.1.2. *Pulsating follower force*

In this study, the constant component of the follower force is set to 10% of the critical load of a beam without a crack. Figure 10 shows the instability boundary curves, and the region between the two curves indicates the instability region due to the parametric

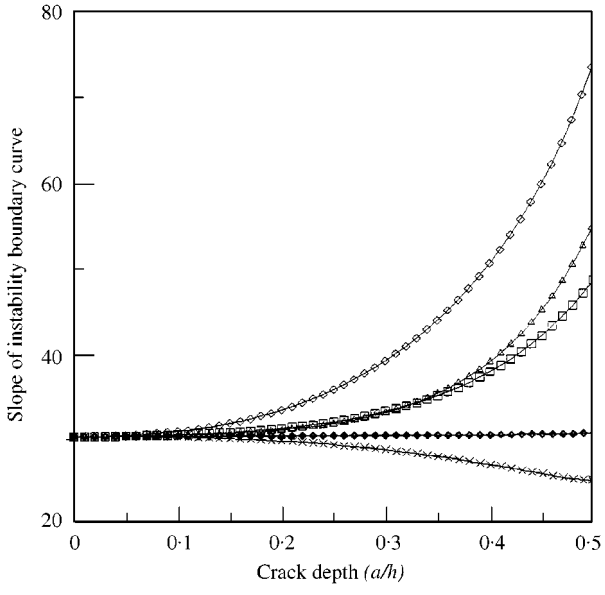

Figure 11. Variation of slope of stability boundary curve around $2\omega_1$. Location of crack (x_c/L): —◆— 0·1; —□— 0·3; —◇—0·5; —△— 0·7; —×— 0·9.

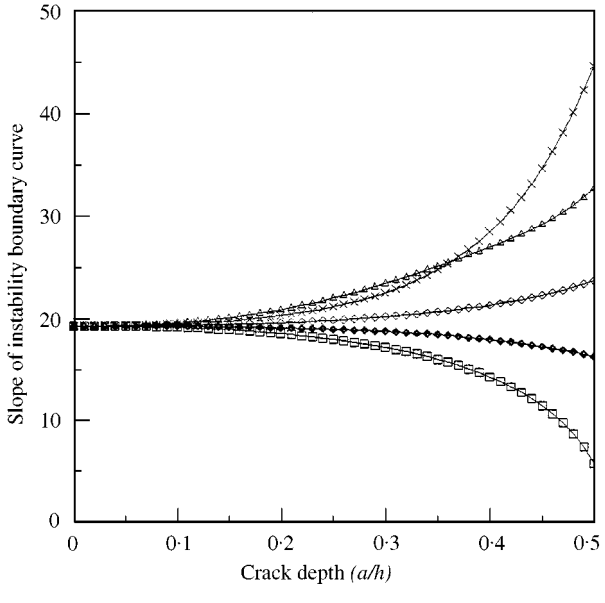

Figure 12. Variation of slope of stability boundary curve around ω_2–ω_1. Location of crack (x_c/L): —◆— 0·1; —□— 0·3; —◇—0·5; —△— 0·7; —×— 0·9.

resonance. Figure 11 shows the effect of the crack on the slopes of the boundary curves at around $2\omega_1$. Varying the depth of the crack to up to 50% of the diameter of the cross-section, the variations of the slopes are observed. As the crack is positioned near the mid-point of the beam, the increment of the slopes are large. As seen from Figure 12, the

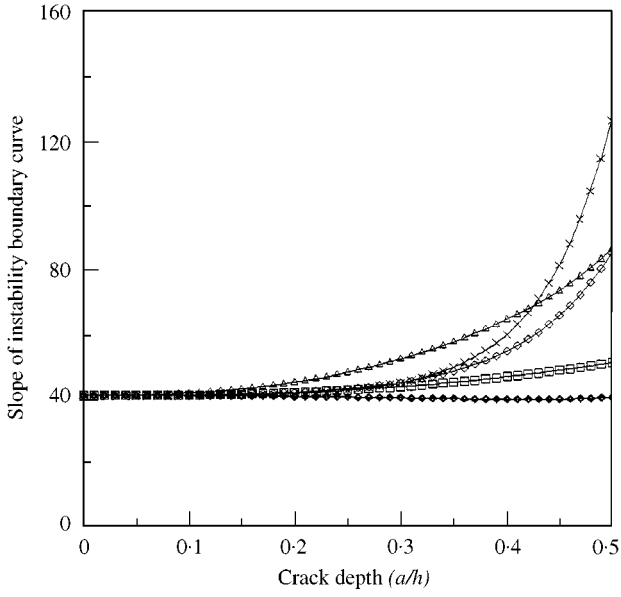

Figure 13. Variation of slope of stability boundary curve around $2\omega_2$. Location of crack (x_c/L): —◆— 0·1; —□— 0·3; —◇—0·5; —△— 0·7; —×— 0·9.

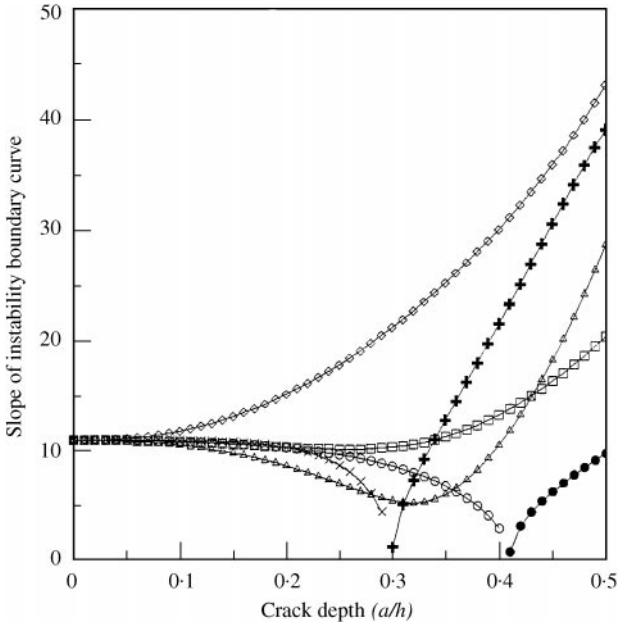

Figure 14. Variation of slope of stability boundary curve around $\omega_1 + \omega_3$. Location of crack (x_c/L): sum type: —○— 0·1; —□— 0·3; —◇—0·5; —△— 0·7; —×— 0·9; (difference-type): —●— 0·1; —+— 0·9.

slopes of the boundary curves around $\omega_2 - \omega_1$ decrease when the crack is located at the front part of the beam. As the crack is located at the latter part of the beam, it induces increment in the slopes. Figure 13 shows the slopes of the boundary curve around $2\omega_2$. The effect of the crack on the increment of the slopes becomes larger as the crack is located in the latter part of the beam. Figure 14 shows the case of combination resonance of type $\omega_1 + \omega_3$.

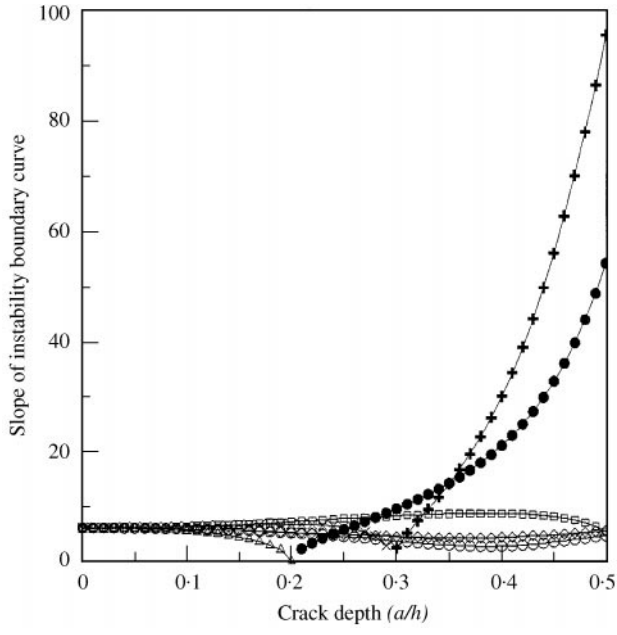

Figure 15. Variation of slope of stability boundary curve around ω_3–ω_2. Location of crack (x_c/L): (difference-type): —○— 0·1; —□— 0·3; —◇—0·5; —△— 0·7; —×— 0·9; (sum-type): —●— 0·7; —+— 0·9.

When there is no crack, combination type is sum-type. However, when the crack is located near the both the end-points of the beam, the resonance changes into the combination type. As seen from Figure 15, the crack located at the latter part of the beam changes the resonance pattern of ω_3 and ω_2 from difference-type to sum-type.

4. CONCLUSION

The effect of the crack on the stability of a free–free beam subjected to a follower force is studied. The decrement of frequencies depends on the position of the crack and the mode shapes. The stability behavior is mainly affected by the location of the crack. We draw the following conclusions:

4.1. CONSTANT FOLLOWER FORCE

When the crack is considerably small, the decrement of the critical load largely depends on the decrement of the second mode frequency, because the instability type is the flutter. As the depth of the crack becomes large, the divergence-type instability occurs when the crack is located at the mid-point or the latter part of the beam, and it results in the sudden drop in the critical load. The crack located at the latter part of the beam causes more decrement of the critical load than the crack located at the front part of the beam.

4.2. PULSATING FOLLOWER FORCE

The effect of the crack on the instability region varies according to the location of the crack. The crack changes not only the slopes of the boundary curve of the parametric resonance but also the resonance type.

REFERENCES

1. V. V. BOLOTIN 1963 *Nonconservative Problems of the Theory of Elastic Stability*. Oxford: Pergamon Press.
2. T. R. BEAL 1965 *American Institute of Aeronautics and Astronautics Journal* **3**, 486–494. Dynamic stability of a flexible missle under constant and pulsating thrusts.
3. J. J. WU 1975 *American Institute of Aeronautics and Astronautics Journal* **14**, 313–319. Missle stability using finite elements—an unconstrained variational approach.
4. K. HIGUCHI 1994 *American Institute of Aeronautics and Astronautics Conference Paper* 1620. An experimental model of a flexible free–free column in dynamic instability due to an end thrust.
5. R. C. KAR and T. SUJATA 1992 *Journal of Sound and Vibration* **154**, 81–93. Stability boundaries of a rotating cantilever beam with end mass under a transverse follower excitation.
6. J. H. KIM and Y. S. CHOO 1998 *Journal of Sound and Vibration* **216**, 623–636. Dynamic stability of a free–free Timoshenko beam subjected to a pulsating follower force.
7. N. ANIFANTIS and A. D. DIMAROGONAS 1983 *International Journal of Structures* **19**, 281–291. Stability of columns with a single crack subjected to follower and vertical load.
8. G. GAUNARIS and A. D. DIMAROGONAS 1988 *Computers and Structures* **28**, 309–313. A finite element of a cracked prismatic beam for structural analysis.
9. R. SUACE, C. ROUTOLO and D. STORER 1996 *Computers and Structures* **61**, 1057–1074. Harmonic analysis of the vibration of a cantilevered beam with a closing crack.
10. G. L. QIAN, S. N. GU and J. S. JIANG 1990 *Journal of Sound and Vibration* **138**, 233–243. The dynamic behaviour and crack detection of a beam with a crack.
11. T. L. ANDERSON 1995 *Fracture Mechanics*. Boca Raton: CRC Press.
12. C. L. DYM and I. H. SHAMES 1973 *Solid Mechanics—A Variational Approach*: *Beams*, *Frames and Rings*. New York: McGraw-Hill, (chapter 4.)
13. J. KOSMATKA 1994 *American Institute of Aeronautics and Astronautics Conference Paper* 1331. Stability and natural frequencies of axial-loaded shear-deformable beams using an improved two-node finite element.
14. A. H. NAYFEH and D. T. MOOK 1979 *Nonlinear Oscillations*: *Parametrically Excited Systems*. New York: John Wiley, (chapter 5.)